熊本大学学術リポジトリ

The Reactor Design for Diesel Exhaust Control Using a Magnetic Pulse Compressor

journal or publication title	IEEE TRANSACTIONS ON PLASMA SCIENCE
volume	32
number	5
page range	2038-2044
year	2004-10
URL	http://hdl.handle.net/2298/3493

doi: 10.1109/TPS.2004.835447

The Reactor Design for Diesel Exhaust Control Using a Magnetic Pulse Compressor

Douyan Wang, *Member, IEEE*, Takao Namihira, *Member, IEEE*, Koji Fujiya, Sunao Katsuki, *Member, IEEE*, and Hidenori Akiyama, *Fellow, IEEE*

***Abstract*—A magnetic pulse compressor (MPC) was used to control the exhaust gases from a diesel generator employing a wire-to-plate plasma reactor in this work. To obtain efficient NO_X removal, the energy transfer efficiency from the MPC to the plasma reactor and the pulse streamer discharge physics were investigated by varying the number of anode wires and wire-to-wire distance of the reactor. It was experimentally confirmed that the number of wires and the neighboring wire distance affected the energy transfer efficiency. The optimal reactor design for efficient diesel exhaust processing using an MPC can be achieved by employing large numbers of wires and long wire-to-wire distances for the wire-to-plate reactor.**

***Index Terms*—Diesel exhaust treatment, energy transfer efficiency, plasma reactor optimization, pulsed streamer discharge.**

I. Introduction

NONTHERMAL plasmas, in which the mean energy of the electrons is substantially higher than that of the ions and the neutrals, offer a major advantage in reducing the energy required to remove pollutants [1]–[4]. The application of short-duration pulsed power to a gaseous gap at atmospheric pressure results in the production of a nonthermal plasma. Applications of pulsed streamer discharges for the removal of $NO_X (= NO + NO_2)$ have been reported at various energy efficiencies [5]–[12]. Also, several techniques have been used for the treatment of diesel exhaust in recent years with various degrees of success [13]–[19].

Increasing the overall energy efficiency of NO_X removal is one of the main objectives directed toward practical applications. The energy transfer efficiency from the pulse generation circuit to the reactor is currently in active development. Although the capacitance of the plasma reactor during streamer discharge development varies from the capacitance before streamer discharge onset [20], [21], the effect of the value of the capacitance before streamer discharge onset was examined by Mok [22]. For a wire-to-plate reactor structure, Mok found that the maximum energy transfer efficiency from the pulse generation circuit to the streamer discharge reactor was achieved when the ratio of the pulse-forming capacitance to the geometric capacitance of the reactor was around 3.0. This is because the capacitance of the reactor increases up to approximately three times due to the streamer development. However, the influence of wire-to-wire distance should be considered since it leads to the change in plasma conditions during the streamer discharge. Kim *et al.* performed two-dimensional time-dependent numerical simulations of the development of a pulsed streamer discharge, and explained that the streamer propagation in a wire-to-plate electrode is strongly influenced by the reactor geometry, particularly, the neighboring wire distance, by illustrating the two-dimensional images of the electron density and electric field intensity [23].

In this work, a magnetic pulse compressor (MPC) has been used to remove NO_X from exhaust of a diesel generator in a wire-to-plate plasma reactor. Understanding pulse streamer discharge physics is an important factor to determine the optimal design parameters of the plasma reactor. In this work, the effects of the number of anode wires and the wire-to-wire distances are investigated in order to obtain high-energy transfer efficiency from pulse generation circuit to the streamer discharge. The optimal reactor design for diesel exhaust treatment is proposed.

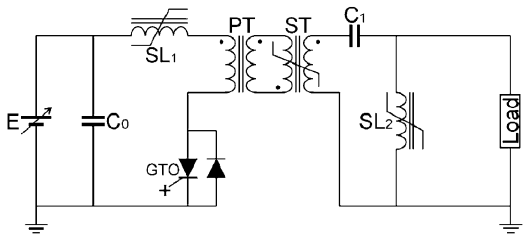

Fig. 1. Schematic diagram of the MPC.

II. Experimental Apparatus and Procedure

Fig. 1 shows the schematic diagram of the MPC used. The MPC consists of a dc power supply, a semiconductor switch, a pulse transformer (PT, ratio, 1:3), a saturable transformer (ST, ratio, 1:8), saturable inductors (SL_1 and SL_2), a low inductance energy storage capacitor ($C_S = 800$ nF), and a low-inductance pulse-forming capacitor ($C_P = 1$ nF). A high-speed gate turn-off thyristor (GTO, H10D33YFH, Meidensha Corp., Japan) was used to switch the primary circuit [24]. The maximum output voltage, maximum pulse repetition rate, and pulse duration of the MPC are 60 kV (positive polarity), 500 pulses per second (pps), and about 130 ns, respectively. The characteristic impedance of the MPC is less than 10 Ω.

Fig. 2 shows the schematic diagram of the wire-to-plate electrode. The diameter of the stainless steel wire was 0.5 mm, and the length and width of the stainless steel plate were 500 and

Manuscript received January 30, 2004; revised March 21, 2004.

D. Wang, T. Namihira, S. Katsuki, and H. Akiyama are with the Department of Electrical and Computer Engineering, Kumamoto University, Kumamoto 860-8555, Japan (e-mail: douyan@st.eecs.kumamoto-u.ac.jp).

K. Fujiya was with with the Department of Electrical and Computer Engineering, Kumamoto University, Kumamoto 860-8555, Japan. He is now with Aishin Seiki Company, Ltd., Aichi, 448-8650 Japan.

Digital Object Identifier 10.1109/TPS.2004.835447

0093-3813/04$20.00 © 2004 IEEE

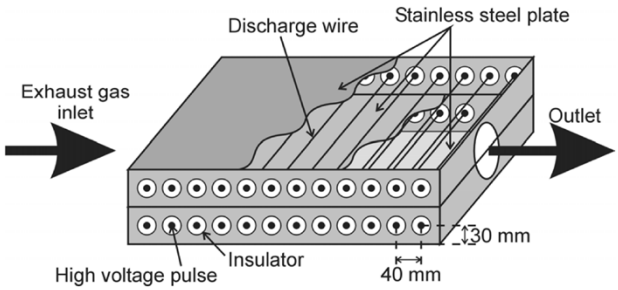

Fig. 2. Schematic diagram of the wire-to-plate electrode.

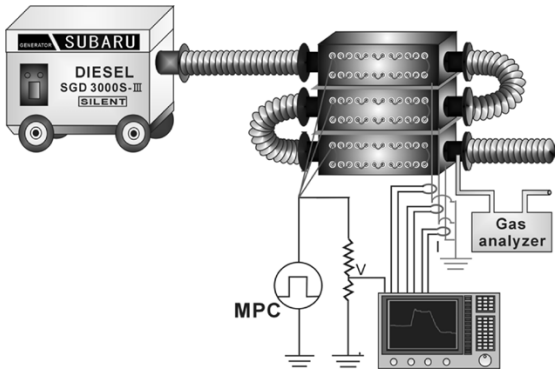

Fig. 3. Experimental set up for treatment of diesel generator exhaust using the wire-to-plate plasma reactor.

300 mm, respectively. Three plates were placed parallel to each other. The distance between each neighboring plate was fixed at 60 mm. The wires were arranged in the center of each neighboring plates and electrically connected to one another. Consequently, the air gap between the wire and plate was 30 mm. The distance between neighboring wires was adjustable by 40 mm increments (40, 80, or 120 mm). The maximum number of wires in the wire-to-plate electrode was 24 with the wire-to-wire distance of 40 mm. The positive high voltage pulses were applied to the wire, and the plates were grounded. Therefore, the wires and plates acted as the anode and cathode, respectively.

Fig. 3 shows the experimental set up for NO_X removal in this work. Three of the wire-to-plate electrodes were connected in series and were employed as a plasma reactor to remove NO_X from the diesel generator exhaust. The diesel generator (SGD 3000S-III, 3.2 kW, SUBARU, Japan) was driven at 2.38 kW for all experiments. The exhaust gas containing NO_X flowed from the generator to the plasma reactor. The gas flow rate was 236.7 $\mathrm{l/min}$. The gas temperatures at the inlet and the outlet of the plasma reactor were 411 K and 318 K, respectively. The MPC was used to generate the streamer discharge in the plasma reactor. The positive pulse voltage repetitive rate from the MPC applied to the plasma reactor was between 100 to 400 pps. The applied voltage to the plasma reactor was measured using a resistive voltage divider (ratio: 20×10^3, rise time: 20 ns, maximum bandwidth: 90 MHz), which was connected between the positive anode wire and the ground cathode plate. The current into the plasma reactor was measured using three current monitors (Pearson current monitor, Model 2878, Pearson Electronics), which were located on the return line to the ground. A digital oscilloscope (HP 54 542A, Hewlett Packard) with a maximum bandwidth of 500 MHz and a maximum sample rate of 2 Gsamples/s recorded the signals from the voltage divider and the current transformers. The concentrations of NO and NO_2 were measured using a gas analyzer (Testo 350, Hodakatest, Japan) after achieving steady state for each experimental condition. The gas analyzer is based on potentiostatic electrolysis. The influences of oxidant gases, such as ozone, were correct within 3% for the concentrations of NO and NO_2 measured.

In the present work, the peak of the pulse voltage applied to the plasma reactor was maintained constant for all experiments by adjusting the charging voltage to the C_S in the primary circuit of MPC. To measure the capacitance of the plasma reactor before streamer discharge onset, the applied voltage and current into the reactor were measured at low applied voltage without a streamer discharge. In this case, the single pulse was applied to the plasma reactor, and both the applied voltage and discharge current were averaged based on 15 waveforms to obtain accuracy. In this work, two attempts are discussed in order to obtain an optimal reactor design for efficient diesel exhaust control using the MPC.

A. *Effects of Number of Wires*

To understand the effect of the length of the discharge wires, the number of discharge wires (either 24 or 48) was set with a constant wire-to-wire distance of 40 mm in the wire-to-plate reactor. Therefore, the larger number of discharge wires provides a longer processing time of the exhaust gases in the plasma reactor. In fact, the gas processing times in the reactor at the flow rate 236.7 $\mathrm{l/min}$ were 4.56 and 9.12 s for 24 and 48 wires, respectively.

B. *Effects of Wire-to-Wire Distance*

To understand the effect of wire-to-wire distance in the wire-to-plate reactor on NO_X removal, the different wire-to-wire distances were examined. The total number of discharge wires in the reactor was fixed at 24, and the wire-to-wire distance was adjusted to 40, 80, or 120 mm, respectively. Therefore, the effective length of discharge wires in reactor is the same for all cases in this experiment. The discharge wire densities between the neighboring plates of the plasma reactor were 25.0, 12.5, and 8.3 wires/m for the wire-to-wire distance of 40, 80, and 120 mm, respectively. The gas processing times in the reactor were 4.56, 9.12, and 13.7 s for 40, 80, and 120 mm, respectively.

III. Results and Discussions

A. *Effects of Number of Wires*

Fig. 4 shows the typical waveforms of the applied voltage and discharge current to the plasma reactor for different numbers of anode wires. The peak value of the applied voltage was 42.4±0.1 kVfor both cases. The negative voltage swing following the positive peak was due to oscillations between the inductance, SL_2, of the MPC and the capacitance of the plasma reactor. The peak current was 279 and 559 A for 24 and 48 wires, respectively. The input energy to the plasma reactor per pulse was calculated from the voltage and the current waveforms in

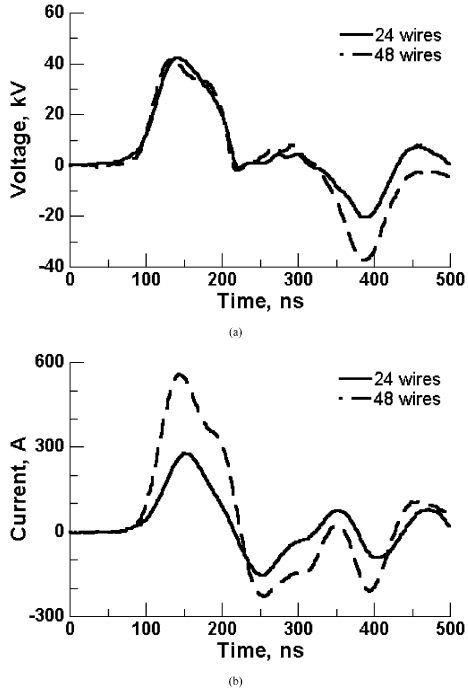

Fig. 4. Typical waveforms of (a) the applied voltage and (b) discharge current in the plasma reactor for different numbers of wires.

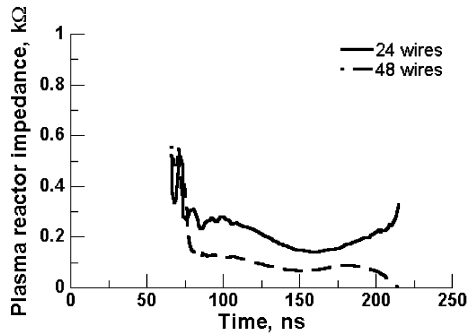

Fig. 5. Plasma reactor impedance during discharge for different numbers of wires.

Fig. 4, and the calculated energies were 0.67 and 1.44 J/pulse for 24 and 48 wires, respectively. Fig. 5 shows the plasma reactor impedance calculated from the voltage and current waveforms in Fig. 4. As shown in Fig. 5, the impedance of the plasma reactor decreased with increasing number of wires during the discharge period. This is because a larger number of streamers were produced and a larger current flowed with an increasing effective length of anode wires.

Fig. 6 shows the dependence of the NO_X removal ratio on the power consumption of the MPC for different numbers of wires. The power consumption of the MPC (P_{in}, in W) is given by following equations:

$$P_{in} = f \times E_{ch} \tag{1}$$

$$E_{ch} = \frac{1}{2} C_S V_{ch}^2 \tag{2}$$

where f (in pps), E_{ch} (in J/pulse), and V_{ch} (in V) are the pulse repetition rate, the storage energy, and the charging voltage of

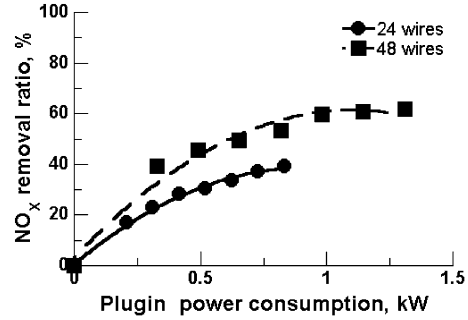

Fig. 6. Dependence of the NO_X removal ratio on the power consumption of the MPC for different numbers of wires.

TABLE I
PLASMA REACTOR IMPEDANCE, Z_R, PLASMA REACTOR CAPACITANCE BEFORE STREAMER DISCHARGE ONSET, C_{R0}, ENERGY TRANSFER EFFICIENCY FROM THE MPC TO THE PLASMA REACTOR, E_T, AND NO_X REMOVAL RATIO AT 0.80 KW OF P_{IN}, NO_{XR}, FOR DIFFERENT NUMBERS OF WIRES

Number of Wires	24 wires	48 wires
Z_R [Ω]	Z_{R24}	Z_{R48} ($Z_{R48} < Z_{R24}$)
C_{R0} [pF]	180	360
E_T [%]	30.0	44.0
NO_{XR} [%]	44.0	57.0

C_S of the MPC for a single pulse, respectively. The removal ratio of NO_X (NO_{XR}, in %) is given by

$$NO_{XR} = \frac{NO_{Xi} - NO_{Xf}}{NO_{Xi}} \times 100 \tag{3}$$

where NO_{Xi} (in ppm) and NO_{Xf} (in ppm) are the initial and the final concentrations of NO_X in the exhaust gas, respectively. Fig. 6 shows that the NO_X removal ratio increased with increasing power consumption and increasing the number of discharge wires. Since the larger number of discharge wires allows the exhaust gases to process for a longer time in the discharge region, a larger number of collisions between the high-energy electrons and the ambient gases, such as N_2, O_2, and H_2O, in the streamers takes place and produces more O, N, and OH radicals [12]. These radicals are well known as reducing agents for NO and NO_2 molecules [5]. Moreover, the larger number of streamers, resulting in higher power consumption (= higher repetition), makes it possible to remove greater amounts of NO_X.

Table I shows the plasma reactor impedance, plasma reactor capacitance before streamer discharge onset, energy transfer efficiency from the MPC to the plasma reactor, and the NO_X removal ratio at 0.80 kW of P_{in} for different numbers of wires. The plasma reactor capacitance before streamer discharge onset (C_{R0}) is given by

$$C_{R0} = \frac{\int_0^t i dt}{V_t} \tag{4}$$

where V_t (in V) and i (in A) are the applied voltage at certain time (t) and the current into the reactor, under low applied voltage conditions that do not cause a streamer discharge in the

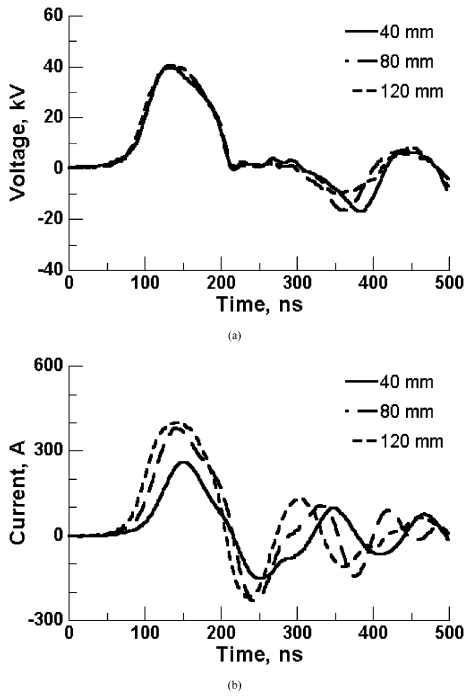

Fig. 7. Typical waveforms of (a) the applied voltage and (b) discharge current in the plasma reactor for different wire-to-wire distances.

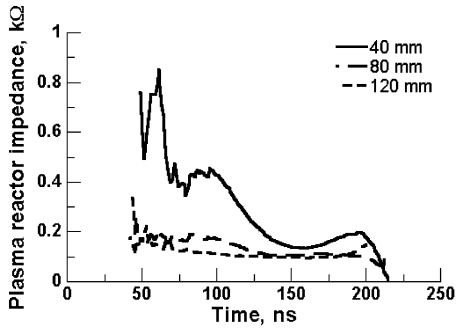

Fig. 8. Plasma reactor impedance during discharge for different wire-to-wire distances.

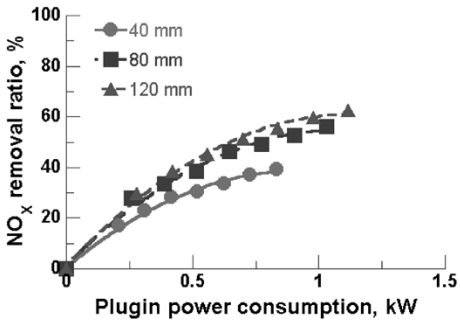

Fig. 9. Dependence of the NO_X removal ratio on the power consumption of the MPC for different wire-to-wire distances.

plasma reactor. The energy transfer efficiency (E_T, %) is calculated from the input energy to the plasma reactor divided by the storage energy in C_S of the MPC (E_{ch}) for a single pulse.

Table I indicates that the NO_X removal ratio is higher at high-energy transfer efficiency. The energy transfer efficiency improved with decreasing plasma reactor impedance and increasing plasma reactor capacitance before streamer discharge onset. Since the output characteristic impedance of MPC is less that 10 Ω, this result suggests that the lower impedance of the plasma reactor results in a better impedance match with the MPC, thus yielding higher energy transfer efficiency. According to Mok [22], the energy transfer efficiency from the pulse generation circuit to the streamer discharge reactor shows a maximum when the ratio of the pulse-forming capacitance to the geometric capacitance of the reactor was around 3.0. In Table I, the plasma reactor capacitance before streamer discharge onset in case of 48 wires was 360 pF, which is around 1/3 value of the pulse-forming capacitance, C_P, yielding higher energy transfer efficiency. This result is in good agreement with Mok's data.

B. Effects of Wire-to-Wire Distance

Fig. 7 shows the typical waveforms of the applied voltage and the discharge current for different neighboring wire-to-wire distances. The peak value of the applied voltages was 40.1±0.4 kV for all cases. The peak current was 260, 375, and 399 A for 40, 80, and 120 mm wire-to-wire distances, respectively. The calculated input energy to the plasma reactor was 0.60, 1.01, and 1.17 J/pulse, respectively. The characteristics of these waveforms as shown in Fig. 8 indicate that the impedance during the discharge period of the plasma reactor decreases with increasing wire-to-wire distance.

Fig. 9 shows the dependence of the NO_X removal ratio on the power consumption of MPC for different wire-to-wire distances. It can be observed from Fig. 9 that the NO_X removal ratio increased with increasing power consumption for a constant neighboring wire distance. This is because, as mentioned with reference to Fig. 6, the larger number of streamers resulted in higher power consumption making it possible to remove greater amounts of NO_X. Fig. 9 also shows that the removal ratio of NO_X increased with increasing neighboring wire distance for constant power consumption. The longer distance between wires in the reactor resulted in longer gas processing time makes the radicals produced in the streamer discharges react more effectively with the NO_X molecules. This can be one reason for higher removal efficiency of NO_X with longer wire-to-wire distances. Another possible reason is presented in Table II.

TABLE II
PLASMA REACTOR IMPEDANCE, Z_R, THE PLASMA REACTOR CAPACITANCE BEFORE STREAMER DISCHARGE ONSET, C_{R0}, ENERGY TRANSFER EFFICIENCY FROM THE MPC TO THE PLASMA REACTOR, E_T, AND NO_X REMOVAL RATIO AT 0.80 KW OF P_{IN}, NO_{XR}, FOR DIFFERENT WIRE-TO-WIRE DISTANCES

Wire-to-Wire Distance	40 mm	80 mm	120 mm
Z_R [Ω]	Z_{R40}	Z_{R80} ($Z_{R80} < Z_{R40}$)	Z_{R120} ($Z_{R120} < Z_{R80} < Z_{R40}$)
C_{R0} [pF]	180	184	195
E_T [%]	28.8	39.1	41.9
NO_{XR} [%]	38.0	51.0	56.0

Table II shows the same representations as Table I for different wire-to-wire distances. The calculation methods for Z_R, C_{R0}, and E_T are the same as in Table I. The plasma reactor capacitance before streamer discharge onset in Table II shows a

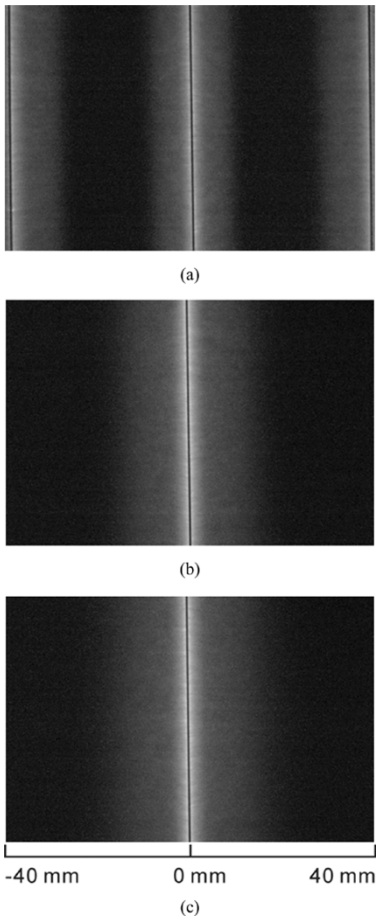

Fig. 10. Typical images of a pulsed streamer discharge for (a) 40, (b) 80, and (c) 120 mm wire-to-wire distances.

similar value for different wire-to-wire distances since the effective length of total wires is same for all cases. From Table II, it is clear that higher energy transfer efficiency is obtained by increasing wire-to-wire distance, which yields a higher NO_X removal ratio. In contrast with Table I, the energy transfer efficiency was influenced by the difference of the wire-to-wire distance even though C_{R0} is the same. This means that the plasma during the discharge period changed by varying the wire-to-wire distances.

To evaluate the discharge condition with varying distance between neighboring wires, time integrated images of pulsed streamer discharges for three wire-to-wire distances were taken from the top view of the wire-to-plate electrode. In this case, one of the plate electrodes was removed to take the images. Fig. 10 shows typical images for 40, 80, and 120 mm wire-to-wire distances. Each image was taken by integrating 2000 pulses for an exposure time of 10 s and pulse repetition rate of 200 pps. From Fig. 10, it is seen that the discharges have bluish emissions and spread out homogeneously, with the strongest emissions observed in the vicinity of the anode wires. The bright emissions around the anode wire are attributed to the secondary streamer discharges which are caused by the strong electric field near the anode wire surface [7].

To visualize the differences between the discharges for each wire-to-wire distance, the images were converted into numerical values (brightness versus position) as shown in Fig. 11.

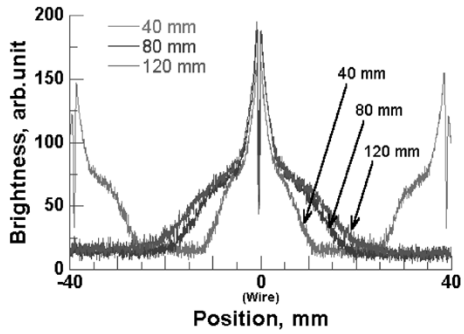

Fig. 11. Dependence of the discharge emission brightness on position for different wire-to-wire distances.

The vertical and horizontal axes of Fig. 11 represent the brightness and lateral distance from the anode wire. Observe from Fig. 11 that the emissions from the streamer discharges spread and became weaker in both directions of the horizontal axis, and the width of the bright area increases with increasing wire-to-wire distance. This result agrees with the simulated result for a pulsed streamer discharge in a wire-to-plate electrode geometry as determined by Kim *et al.* [23]. Kim suggests that as the adjacent wire electrodes are brought closer, their affects on the electric field distribution become stronger and the streamers from adjacent wires consequently shrink to considerably narrow ranges. In the present work, the interference effects of closer wire-to-wire distance are shown in Figs. 10 and 11 and result in a higher impedance during the discharge period due to the decrease in size of the streamers (Table II). In addition, Kim recommended that the wire-to-wire spacing should be at least twice the wire-to-plate distance to produce an effective nonequilibrium plasma for enhancing the efficiency of the exhaust gas cleaning process. As shown in Fig. 9, the dependence of NO_X removal on power consumption is almost the same for both wire-to-wire distances of 80 and 120 mm. According to the recommendation by Kim, this is because both distances are over twice the distance compared to the wire to plate electrodes distance (30 mm), and wide enough to avoid interference effects by neighboring wires.

The results in Section III indicate that the ratio of the pulse-forming capacitance to the geometric capacitance of the reactor is important to obtain the higher energy transfer efficiency from the pulse generation circuit to discharge. Furthermore, the longer distance between wires makes sufficient improvement of NO_X removal using the wire-to-plate electrode.

IV. Conclusion

Pulsed streamer discharges in a wire-to-plate reactor have been used to remove NO_X from diesel generator exhaust gases. The following conclusions have been deduced.

1) For a fixed peak pulse voltage applied to the wire-to-plate plasma reactor, the energy transfer efficiency from the MPC into the streamer discharges increases with increasing number of wires and increasing wire-to-wire distance in the plasma reactor. As a result, the NO_X removal

ratio increases with increasing number of wires and increasing wire-to-wire distance at a constant plug-in power consumption.

2) It was experimentally confirmed that the energy transfer efficiency is higher when the plasma reactor capacitance before plasma onset, C_{R0}, is close to 1/3 value of the pulse-forming capacitance, C_P, of the MPC.
3) The energy transfer efficiency increases with decreasing plasma reactor impedance. The lower plasma reactor impedance is a better impedance match with the MPC thereby improving the energy efficiency of the NO_X removal.
4) At a fixed pulse voltage and fixed number of wires, the streamer discharge volume increased with longer wire-to-wire distance in the wire-to-plate reactor. This is because the longer wire-to-wire distance weakens the influence of overlapped electric field distributions between neighboring wires.
5) For efficient diesel exhaust control using a wire-to-plate reactor with an MPC, it is important to obtain a better impedance match between the MPC and the plasma reactor by employing large numbers of wires and long wire-to-wire distances. Also, it is good to have an appropriate ratio of C_{R0} and C_P.

In this work, the results of NO_X removal on power consumption leaves room for further improvement to obtain the optimal reactor design for diesel exhaust control using an MPC. Additional improvement techniques to be considered are the application of an optical reactor, a shorter pulse (less than 100 ns), chemical additives (ammonia, etc.), and a catalyst.

REFERENCES

[1] B. M. Penetrante, "Pollution control applications of pulsed power technology," in *9th IEEE Int. Pulsed Power Conf. Dig. Tech. Papers*, Albuquerque, NM, 1993, pp. 1–5.

[2] K. Urashima, J. S. Chang, J. Y. Park, D. C. Lee, A. Chakrabarti, and T. Ito, "Reduction of NO_X from natural gas combustion flue gases by corona discharge radical injection techniques," *IEEE Trans. Ind. Applicat.*, vol. 34, pp. 934–939, Sept.–Oct. 1998.

[3] J. S. Chang, P. A. Lawless, and T. Yamamoto, "Corona discharge process," *IEEE Trans. Plasma Sci.*, vol. 19, pp. 1152–1166, Dec. 1991.

[4] R. McAdams, "Prospects for nonthermal atmospheric plasmas for pollution abatement," *J. Physics D., Appl. Phys.*, vol. 34, pp. 2810–2821, 2001.

[5] R. Hackam and H. Akiyama, "Air pollution control by electrical discharges," *IEEE Trans. Dielectr. Electr. Insul.*, vol. 7, pp. 654–683, Oct. 2000.

[6] B. M. Penetrante, M. C. Hsiao, B. T. Merritt, G. E. Vogtlin, and P. H. Wallman, "Comparison of electrical discharge techniques for nonthermal plasma processing of NO and NO_2," *IEEE Trans. Plasma Sci.*, vol. 23, pp. 679–687, Aug. 1995.

[7] T. Namihira, D. Wang, S. Katsuki, R. Hackam, and H. Akiyama, "Propagation velocity of pulsed streamer discharges in atmospheric air," *IEEE Trans. Plasma Sci.*, vol. 31, pp. 1091–1094, Oct. 2003.

[8] E. M. van Veldhuizen, W. R. Rutgers, and V. A. Bityurin, "Energy efficiency of NO removal by pulsed corona discharges," *Plasma Chem. Plasma Process.*, vol. 16, pp. 227–247, 1996.

[9] T. Namihira, S. Tsukamoto, D. Wang, S. Katsuki, R. Hackam, H. Akiyamma, Y. Uchida, and M. Koike, "Improvement of NO_X removal efficiency using short width pulsed power," *IEEE Trans. Plasma Sci.*, vol. 28, pp. 434–442, Apr. 2000.

[10] S. Tsukamoto, T. Namihira, D. Wang, S. Katsuki, R. Hackam, H. Akiyama, A. Sato, Y. Uchida, and M. Koike, "Effects of fly ash on NO_X removal by pulsed streamers," *IEEE Trans. Plasma Sci.*, vol. 29, pp. 29–36, Feb. 2001.

[11] T. Namihira, D. Wang, S. Tsukamoto, S. Katsuki, and H. Akiyama, "Effect of gas composition for NO_X removal using pulsed power" (in Japanese), *IEEJ Trans. FM* , vol. 119, no. 10, pp. 1190–1195, 1999.

[12] T. Namihira, S. Tsukamoto, D. Wang, H. Hori, S. Katsuki, R. Hackam, H. Akiyama, M. Shimizu, and K. Yokoyama, "Influence of gas flow rate and reactor length on NO removal using pulsed power," *IEEE Trans. Plasma Sci.*, vol. 29, pp. 592–598, Aug. 2001.

[13] B. M. Penetrante, "Removal of NO_X from diesel generator exhaust by pulsed electron beams," in *11th IEEE Int. Pulsed Power Conf. Dig. Tech. Papers*, Baltimore, MD, 1997, pp. 91–96.

[14] K. Takaki and T. Kujiwara, "Multipoint barrier discharge process for removal of NO_X from diesel engine exhaust," *IEEE Trans. Plasma Sci.*, vol. 29, pp. 518–523, June 2001.

[15] M. G. Grothaus, M. K. Khair, and P. Paul, "A synergistic approach for the removal of NO_X and PM from diesel engine exhaust," in *12th IEEE Int. Pulsed Power Conf. Dig. Tech. Papers*, vol. 1, 1999, pp. 506–510.

[16] B. S. Rajanikanth and V. Ravi, "Pulsed electrical discharge assisted by dielectric pellets/catalysts for diesel engine exhaust treatment," *IEEE Trans. Dielectr. Electr. Insul.*, vol. 9, pp. 616–626, Aug. 2002.

[17] Y. Yoshioka, T. Yukitake, M. Nakai, K. Souma, K. Tuchiya, K. Annou, and Y. Hori, "Design and testing of a prototype De-NO_X system for 100 kVA diesel engine generator using a silent discharge reactor," *Combustion Sci. Technol.*, pp. 22–23, 1998.

[18] S. E. Thomas, A. R. Martin, D. Raybone, J. T. Shawcross, K. L. Ng, P. Beech, and J. C. Whitehead, "Non thermal plasma aftertreatment of particulates—Theoretical limits and impact of reactor design," in *Society of Automotive Engineers Spring Fuels and Lubricants Meeting*, Paris, France, 2000, SAE Paper 2000-01-1926.

[19] A. Mizuno, A. Chakrabarti, and K. Okazaki, "Application of corona technology in the reduction of greenhouse gases and other gaseous pollutants," in *Non-Thermal Plasma Techniques for Pollution Control*. ser. NATO ASI, B. M. Penetrante and S. E. Schultheis, Eds. Berlin, Germany: Springer-Verlag, 1993, pt. B, vol. G 34, pp. 165–186.

[20] L. Civitano, "Industrial application of pulsed corona processing to flue gas," in *Non-Thermal Plasma Techniques for Pollution Control*. ser. NATO ASI, B. M. Penetrante and S. E. Schultheis, Eds. Berlin, Germany: Springer-Verlag, 1993, pt. B, pp. 103–130.

[21] H. S. Uhm and W. M. Lee, "An analytical theory of corona discharge plasmas," *Phys. Plasmas*, vol. 4, no. 9, pp. 3117–3128, 1997.

[22] Y. S. Mok, "Efficient energy delivery condition from pulse generation circuit to corona discharge reactor," *Plasma Chem. Plasma Process.*, vol. 20, no. 3, pp. 353–364, 2000.

[23] Y. H. Kim and S. H. Hong, "Two-dimensional simulation images of pulsed corona discharge in a wire-plate reactor," *IEEE Trans. Plasma Sci.*, vol. 30, pp. 168–169, Feb. 2002.

[24] T. Sakugawa, D. Wang, K. Shinozaki, T. Namihira, S. Katsuki, and H. Akiyama, "Repetitive short-pulsed generator using MPC and blumlein line," in *14th IEEE Int. Pulsed Power Conf. Dig. Tech. Papers*, vol. 1, Dallas, TX, 2003, pp. 657–660.

Douyan Wang (M'04) was born in Beijing, China, on May 18, 1975. She received the B.S. and M.S. degrees from Kumamoto University, Kumamoto, Japan, in 1998 and 2000, respectively, where she is currently pursuing the Ph.D. degree.

From 2000 to 2002, she was with Hitachi, Ltd., Ibaraki, Japan. From November 2003 to March 2004, she was on sabbatical leave at the Center for Pulsed Power and Power Electronics, Texas Tech University, Lubbock.

Ms. Wang has been a Japan Society for the Promotion of Science (JSPS) Research Fellow since 2003.

Takao Namihira (M'00) was born in Shizuoka, Japan, on January 23, 1975. He received the B.S., M.S., and Ph.D. degrees from Kumamoto University, Kumamoto, Japan, in 1997, 1999, and 2003. respectively.

Since 1999, he has been a Research Associate at Kumamoto University. He has been on sabbatical leave at the Center for Pulsed Power and Power Electronics, Texas Tech University, Lubbock.

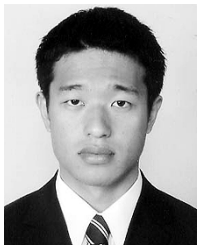

Koji Fujiya was born in Fukuoka, Japan, on October 4, 1979. He received the B.S. and M.S. degrees from Kumamoto University, Kumamoto, Japan, in 2002 and 2004, respectively.

Since 2004, he has been with Aishin Seiki Company, Ltd., Japan.

Sunao Katsuki (M'99) was born in Kumamoto, Japan, on January 5, 1966. He received the B.S., M.S., and Ph.D. degrees from Kumamoto University, Kumamoto, Japan, in 1989, 1991, and 1998, respectively.

From 1991 to 1998, he was a Research Associate at Kumamoto University. Since 1998, he has been an Associate Professor at Kumamoto University.

Hidenori Akiyama (M'87–SM'99–F'00) was born in Ehime, Japan, on April 2, 1951. He received the B.S. degree in electrical engineering from the Kyusyu Institute of Technology, Fukuoka, Japan, in 1974 and the M.S. and Ph.D. degrees from Nagoya University, Nagoya, Japan, in 1976 and 1979, respectively.

From 1979 to 1985, he was a Research Associate at Nagoya University. In 1985, he joined the faculty at Kumamoto University, Kumamoto, Japan, where he is currently a Professor.

Dr. Akiyama received the IEEE Major Education Innovation Award in 2000 and the IEEE Peter Haas Award in 2003.